

PAPER • OPEN ACCESS

Decoration of wide bandgap semiconducting materials for enhancing photoelectrochemical efficiency of PEC systems.

To cite this article: N Bakranov *et al* 2018 *J. Phys.: Conf. Ser.* **987** 012028

View the [article online](#) for updates and enhancements.

Related content

- [ZnO based heterojunctions and their application in environmental photocatalysis](#)
Xiuquan Gu, Cuiyan Li, Shuai Yuan et al.
- [ZnO nanorod/CdS nanocrystal core/shell-type heterostructures for solar cell applications](#)
Gariné Guerguerian, Fernando Elhordoy, Carlos J Pereyra et al.
- [The effect of silver nanoparticles/graphene-coupled TiO₂ beads photocatalyst on the photoconversion efficiency of photoelectrochemical hydrogen production](#)
Chun-Ren Ke, Jyun-Sheng Guo, Yen-Hsun Su et al.



IOP | ebooks™

Bringing you innovative digital publishing with leading voices to create your essential collection of books in STEM research.

Start exploring the collection - download the first chapter of every title for free.

Decoration of wide bandgap semiconducting materials for enhancing photoelectrochemical efficiency of PEC systems.

N Bakranov¹, A Zhabaikhonov¹, S Kudaibergenov¹ and N Ibraev²

¹ Kazakh National Research Technical University after K I Satpayev, Almaty, Kazakhstan

² The Karaganda State University of the name of academician E A Buketov, Karaganda, Kazakhstan

E-mail: bakranov@gmail.com

Abstract. The production of photoanodes based on wide-band gap materials such as TiO₂ is economically viable because of the low cost of synthesis methods. Contrary to economic aspects, wide-band gap semiconductor materials have a significant disadvantage due to low sensitivity to photons of visible light. To increase the photoactive parameters of the material of the electrodes in the visible range, the methods for decorating nanomasses of titanium dioxide by narrow-gap semiconductors are used. One of the most suitable narrow-gap semiconductor materials are CdS and Fe₂O₃. Controlled deposition of such materials on wide-gap semiconductors allows to regulate both the diffusion time of charge carriers and the band structure of TiO₂/Fe₂O₃ and TiO₂/CdS composites. The dimensions of the structure of the photoelectrode material of the cell have a large influence on the characteristics of the photocatalyst created. Thus, in the hematite structures of nanometre dimension, the rate of recombination of charge carriers fades away in comparison with bulk structures. Reducing the size of CdS structures also positively affects the nature of the photocatalytic reaction.

1. Introduction

Sunlight and water are the most common sources of clean renewable energy on Earth [1]. The Sun as a source of electromagnetic waves refers to inexhaustible natural resources, so the use of solar radiation is a key direction of alternative energy today. The power of solar energy incident on the earth's surface at any time is 130 million 500 MW [2]. Water splatted by the action of sunlight, is an inexhaustible source of hydrogen, the production of which belongs to one of the most important criteria of hydrogen energy. The main factor in the production of hydrogen from water under the action of photons is the maximum absorption of photocatalytic materials falling on the Earth's surface (4% ultraviolet (UV), 46% visible, 50% infrared spectrum). Among the developed methods of extracting hydrogen fuel by means of photon energy, the method of photocatalytic water splitting is one of the most promising. The use of widely distributed elements in the earth's crust to create photoactive systems absorbing a wide spectrum of solar radiation will solve the main problem of hydrogen evolution from water. As a result of photocatalytic decomposition of water, light energy is converted into chemical energy, breaking the energy barrier, with a large positive change in free energy Gibbs ($\Delta G = 238$ kJ/mole) [3], similar to the process of energy transformations in the photosynthesis of green plants [4]. Photocatalysts based on widely distributed elements have semiconductor properties. Such semiconductors have a large band gap, the photoabsorption capacity of which lies in the UV range. Thus, there are a number of challenges to



researchers developing systems consisting of low-cost materials capable of exhibiting photocatalytic properties in a wide light range.

The semiconductor materials used in photocatalytic reactions with hydrogen evolution make important demands on the potentials of the levels of the conduction and valence bands. Thus, to realize the half-reaction of the decomposition of water, which consists in the reduction of H^+ to H_2 , the potential of the conduction band of the semiconductor should be more negative than the level of hydrogen evolution ($E_{(H_2/H_2O)}$). While the half-reaction of the oxidation of the water molecule occurs under the condition of the position of the valence band potential in a more positive value of the oxygen release level ($E_{(O_2/H_2O)}$) [5]. Therefore, complete photoelectrochemical splitting of water by semiconductor photocatalysts is realized by using materials of potential regions of conductivity that are more negative than the level of water recovery and potentials of valence bands of more positive levels of water oxidation. The photocatalytic release of hydrogen from water occurs as a result of an oxidation-reduction reaction that occurs both on the surfaces of photocatalytic particles (powder) dispersed in water (electrolyte) and on the surfaces of photoelectrodes. Consequently, two types of photocatalytic systems of water splitting are distinguished: photoelectrochemical and photochemical cells [1].

The photocatalysis process on semiconductor materials includes the following steps:

- 1) absorption of photons of light whose energy is equal to or greater than the width of the forbidden band of the semiconductor, which leads to the generation of an electron-hole pair (excitons) in the semiconductor material;
- 2) rupture of the exciton by migration of photoinduced charge carriers to the surface of the material;
- 3) carrying out the oxidation-reduction reaction by charge carriers of the water molecule [6].

Since the first successful photoelectrochemical splitting of water, performed by Honda and Fujishima in the early 1970s [1], a wide range of materials exhibiting photocatalytic activity has been developed. According to the properties of electronic configurations, such materials form four groups: 1) metal oxides with the configuration $d0$, such as Zr^{4+} , Nb^{5+} , Ta^{5+} , W^{6+} , Mo^{6+} and Ti^{4+} ; 2) metal oxides with a configuration $d10$ (Zn^{2+} , Ga^{3+} , Ge^{4+} , Sn^{4+} , Sb^{5+} and In^{3+}); 3) metal oxides with the configuration $f0$, for example, Ce^{4+} ; 4) non-oxide photocatalysts (Ta_3N_5 , CdS) [2, 3]. Metal oxides, such as TiO_2 , ZnO , Fe_2O_3 , etc., are widely used as the main material of photoanodes of catalytic systems [4].

Titanium dioxide is a wide-band semiconductor material, the photosensitivity of which lies in the UV region. Based on the fact that an insignificant part of the UV spectrum of solar radiation falls to the Earth's surface (about 4%), titanium dioxide has a low level of absorption of light passing through the layers of the atmosphere. Despite the low photosensitivity, TiO_2 is a promising photocatalytic material due to its physicochemical properties - high chemical resistance, low photocorrosion. The process of photocatalytic decomposition of water by dioxide is initiated by the absorption of a photon with an energy equal to or greater than the width of the forbidden band of the semiconductor. After electron irradiation, electron-hole pairs are formed. The photogenerated electrons migrated to the conduction band perform the function of the reducing agent H^+ to H_2 , and the holes migrating to the surface of the semiconductor decompose H_2O to O_2 and H^+ .

By using the evaluation of the operation of a photoelectrochemical or photochemical cell by direct measurement of the quantum yield, it is necessary to take into account both the exact volume of the released gas and the exact number of photons incident on the photocatalyst, which under real conditions is hard to reproduce. It is convenient to evaluate the photoelectrochemical or photochemical system by measuring the so-called photocatalytic efficiency η . The photocatalytic efficiency η of the electrochemical system is calculated by the formula:

$$\eta = \frac{((1.229V - V_b)J)}{P} \quad (1),$$

1.229V is the standard potential needed to separate molecular hydrogen and oxygen from water, V_b is the bias voltage supplied by the external power source, J is the current density through the photoelectrochemical cell (A/m^2), and P is the power of the electromagnetic radiation emitted by the light source (W/m^2) [5].

Experimental data obtained during the decomposition of water by low-dimensional titanium dioxide showed the efficiency of the process of a component of the order of 0.4% when the material was irradiated with a light source with a filter of 1.5 AM-100mW/cm² [6]. It was found that the size and shape of TiO₂ particles play an important role in the formation of the overall efficiency of the photoelectrochemical cell of hydrogen evolution [7]. For example, nanoparticles of titanium dioxide (a mixture of the anatase and rutile phases) precipitated as a thin film with a thickness of 15µm onto the transparent conducting surface have a photocatalytic activity 10 times lower than in the case of TiO₂ nanotubes having an average length of 3µm [8]. An important factor affecting the photocatalytic activity of a photoelectrode made on the basis of nanotubes or nanorods of titanium dioxide is the length of the structures. This feature is due to the total area of light absorption and the area of contact of the photoelectrode with the electrolyte. The downside of increasing the length of nanotubes is the increase in the path travelled by the charge, hence, the time of electronic transport. In view of the fact that the recombination time of most charge carriers (of the order of 60-80%) in the material of a photocatalyst based on titanium dioxide lies in the nanosecond range [9], an increase in carrier transport time increases the probability of recombination of excitons, whereas with an increase in the path traversed by an electron the probability of particles entering the charge-capture zone increases, which has a negative effect on the photocurrent. The suppression of the number of charge carrier capture zones is achieved by improving the crystallinity of the structures by annealing. The density of the photocurrent passing through the photoelectrochemical cell has a direct effect on the efficiency of the cell.

The creation of composite low-dimensional materials to expand the light sensitivity of wide-gap semiconductors requires the observance of the rules of band transitions between the main and decorating semiconductors, the sequence of layers of the material relative to the incident light, etc. Thus, when choosing a narrow-band semiconductor material, the positions of the Fermi levels and the levels of the valence bands and conduction bands, as well as the type of conductivity. The production of low-dimensional TiO₂/Fe₂O₃ composite materials with a given hierarchy was achieved by decorating the titania nanostructures with hematite particles. The tandem architecture of composite samples was performed taking into account the distributions of the spectral sensitivities of wide-band/narrow-band semiconductors. Thus, the TiO₂ layer absorbing only the UV spectrum was located first relative to the front of the incident light. Thus, a visible part of the light that was not absorbed by the wide-gap semiconductor penetrated the hematite layer to generate additional charge carriers in it. In this paper, the efficiency of the photocatalytic activity of the bare structures of wide-band titanium dioxide and nanocomposites such as TiO₂/Fe₂O₃ and TiO₂/CdS have investigated.

2. Experimental section

Synthesis of low-dimensional TiO₂ rods was performed by a hydrothermal method at a temperature of 180°C for 12 hours. A solution for depositing TiO₂ nanorods onto transparent conductive substrates (FTO glass) was prepared from 30 ml of hydrochloric acid, 30 ml of deionized water and 1 ml of titanium butoxide. After carrying out hydrothermal synthesis, the substrates with the structures deposited on them were washed with distilled water. Further, the obtained samples were annealed at 500°C for 2 hours.

Low-dimensional titanium dioxide films were formed by applying a paste consisting of 0.96g of nanoparticles (25 nm in size) TiO₂, 2 ml of polyethylene glycol to transparent conductive surfaces. After applying the TiO₂ paste layers, the samples were annealed at a temperature of 500°C for 2 hours.

2.1. Decoration of TiO₂ nanostructures by hematite

To obtain a nanosized film of Fe₂O₃, an ethanol solution of 0.02 M FeCl₃ was prepared. The deposition of low-dimensional layers of iron oxide was carried out for 1 minute by precipitation of Fe ions contained solution a rotating substrate at a speed of 1000 rpm. a spin coating method, followed by calcination of the structures at a temperature of 350°C. Calcination of coatings was carried out to remove chlorine and form iron oxide. Thus, up to 5 layers of the film Fe₂O₃ were deposited. An annealing at 450°C, following the deposition of the fifth (last) layer of a narrow-band semiconductor, was carried out to create TiO₂/Fe₂O₃ heterostructures.

After deposition of Fe-containing layers on the surface of nanorods or thin-film TiO₂ layers and subsequent calcination in an oxygen atmosphere, the objects obtained formed a TiO₂/Fe₂O₃ heterostructure.

2.2. Synthesis of TiO₂/CdS heterostructures

Thin films based on TiO₂/CdS composites were obtained by two-step hierarchical deposition of titanium dioxide nanoparticles and subsequent deposition of a CdS layer. The hierarchy of TiO₂/CdS composites is formed both taking into account the absorption by the nanostructures of titanium dioxide of the UV spectrum, and the creation of a narrow-gap semiconductor-electrolyte contact.

Deposition of CdS structures on the surface of TiO₂ nanomass was carried out by immersion of the wedge in a vessel with dissolved 0.2M cadmium nitrate and 0.2M thiourea in ethyl alcohol, followed by calcination of the sample at a temperature of 90°C. The calcination time of the components of the CdS structure was 1 hour. After the formation of the CdS film, the samples were washed in distilled water.

3. Result and discussion

The morphology of the sample obtained by hydrothermal synthesis of titanium dioxide was studied by scanning electron microscopy (figure 1). A uniform array of TiO₂ structures consists of rods, with a diameter of 150-200 nm, mainly directed perpendicular to the substrate.

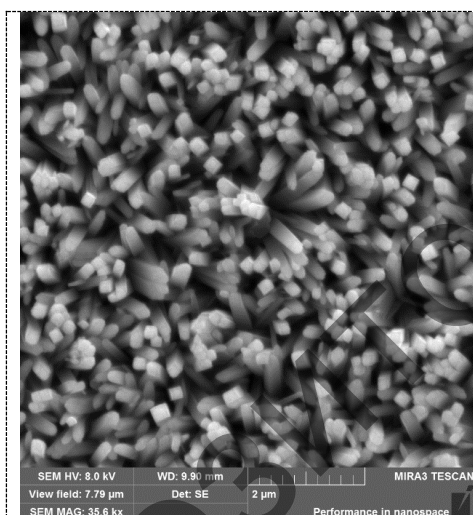


Figure 1. SEM image of nanorods TiO₂ obtained by the hydrothermal method.

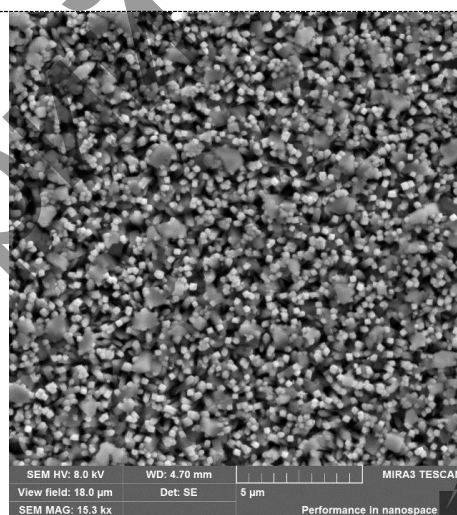


Figure 2. SEM image of a low-dimensional TiO₂/Fe₂O₃ composite

After deposition of Fe-containing layers on the surface of nanorods or thin-film TiO₂ layers and subsequent calcination in an oxygen atmosphere, the objects obtained formed a TiO₂/Fe₂O₃ heterostructure. The morphology of the surface of the resulting nanocomposites is shown in figure 2. The crystals of Fe₂O₃, having an average length of one side of the surface equal to 300 ± 50 nm, are combined on the average with six TiO₂ nanorods, which can facilitate the rapid separation of charge carriers. When carrying out photocatalytic experiments using a photoanode based on TiO₂/Fe₂O₃.

The photocatalytic activity of the obtained materials was studied by a potentiometric method. The photoelectrochemical cell consisted of a platinum cathode, an Ag/AgCl reference electrode, and an anode obtained by depositing semiconductor materials on a conductive glass. The distance between the platinum cathode and the photoanode was 2 cm. The size of the active zone of the photoanode was chosen equal to 1 cm² for a convenient calculation of the current density. For this purpose, an epoxy resin was applied to the entire area, except for a square with a side of 1 cm, a photoelectrode. The contact between the output of the potentiostat and the photoelectrode was produced by graphite glue (figure 3).



Figure 3. Photographic image of the photoanode

When studying the photocatalytic activity of $\text{TiO}_2/\text{Fe}_2\text{O}_3$ composite materials, the increase in the current density of the sample in comparison with the current densities of one-component TiO_2 semiconductors (figure 4) was not detected. The reason for this may be a more positive position of the conductivity level of the narrow-band semiconductor material Fe_2O_3 .

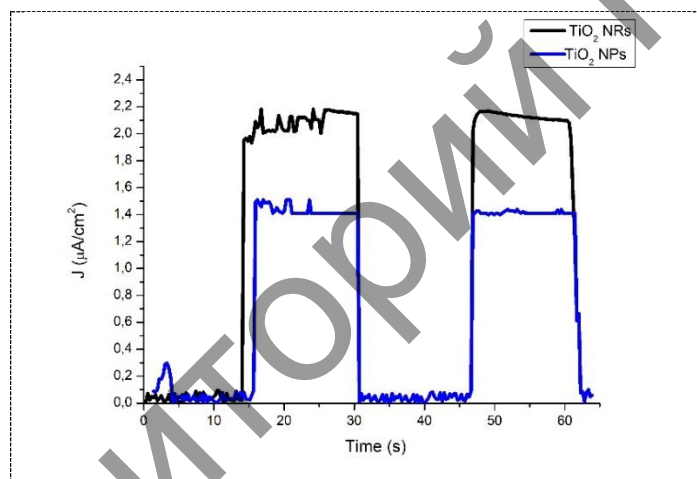


Figure 4. IT diagram of photocurrent curves through low-dimensional TiO_2 systems (NR_s black curve, NP_s blue curve).

The morphology of the coating surface of nanostructures of a wide-gap semiconductor TiO_2 material by a uniform layer of a narrow-gap semiconductor CdS is shown in figure 5. It is understood that the transverse dimension of the formed CdS film exceeds the transverse dimensions of the TiO_2 arrays since The rods and titanium dioxide particles are completely coated with a CdS layer. The dimensions of the particles forming the CdS film averagely 500 nm (figure 5).

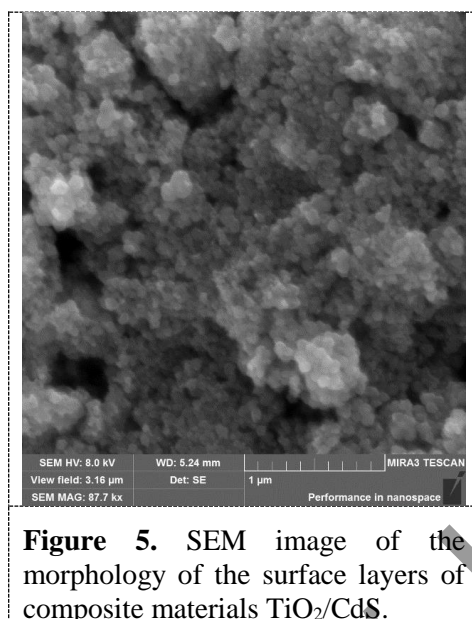


Figure 5. SEM image of the morphology of the surface layers of composite materials TiO_2/CdS .

Energy-dispersive analysis of the samples showed the presence of titanium, oxygen, cadmium and sulphur elements on the composite surface (figure 6). The elements Ca, Si, P, V, identified as a result of EMF analysis, refer to the substrate material.

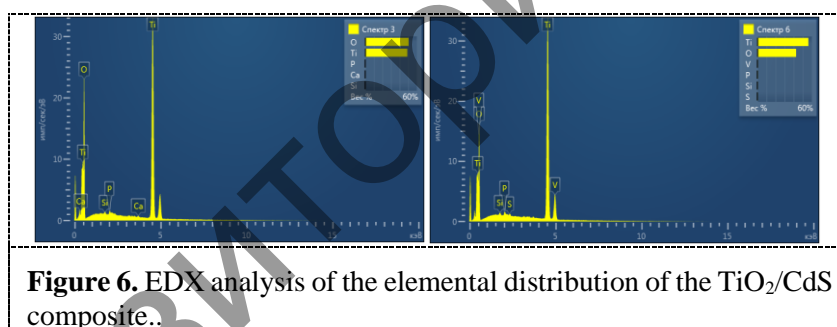


Figure 6. EDX analysis of the elemental distribution of the TiO_2/CdS composite.

Photoelectrochemical measurements of TiO_2/CdS composite materials carried out in potentiostatic mode using distilled water as electrolyte showed a sharp increase in current densities after performing wide-gap semiconductor decorations with low-dimensional CdS layers. At the same time, by depositing CdS particles on the surface of nanorods TiO_2 , the current density of the system increased by an average of 4 times (from $2 \mu\text{A}$ when one-component array was irradiated to $8 \mu\text{A}$ when TiO_2/CdS composites were irradiated). Decoration of nanoparticles by a TiO_2 thin film of CdS made it possible to increase the photocurrent of a photoelectrochemical cell from $1.4 \mu\text{A}$ to $5 \mu\text{A}$ (figure 7). This effect confirms the increase in the photocatalytic activity of the composite photoanode TiO_2/CdS in comparison with the anode made on TiO_2 structures.

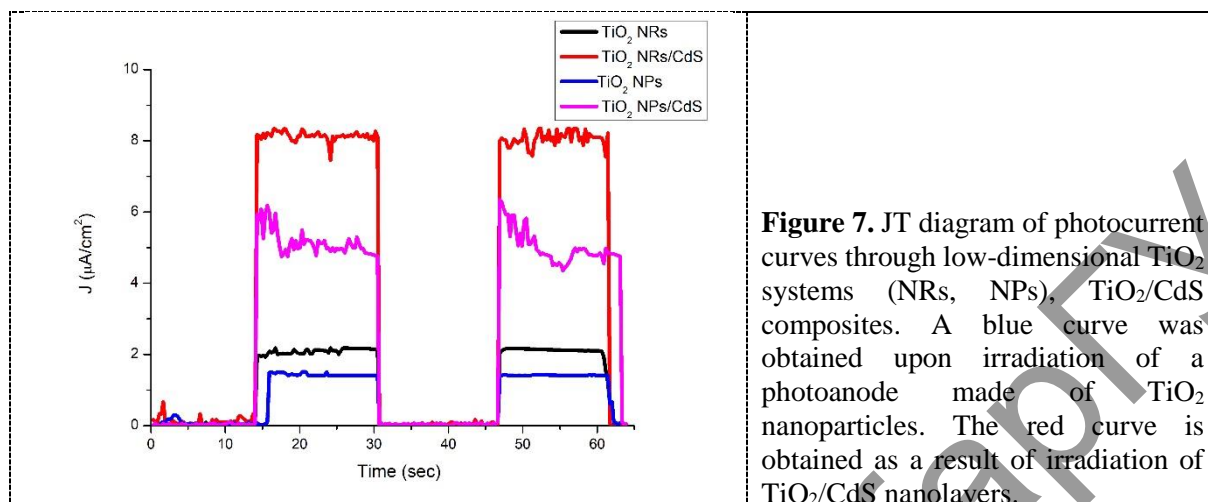


Figure 7. JT diagram of photocurrent curves through low-dimensional TiO₂ systems (NRs, NPs), TiO₂/CdS composites. A blue curve was obtained upon irradiation of a photoanode made of TiO₂ nanoparticles. The red curve is obtained as a result of irradiation of TiO₂/CdS nanolayers.

Calculation of the efficiency of obtained photocathodes

The efficiency of the photocatalytic cell is calculated by the formula (1).

Thus, substituting the values of the current densities J , the experimental efficiency η of the obtained composites is:

$$\eta \text{ TiO}_2/\text{Fe}_2\text{O}_3 = 0.0378;$$

$$\eta \text{ TiO}_2/\text{CdS} = 0.0945-0.1512$$

4. Conclusion

The production of a photoanode based on TiO₂ nanostructures, TiO₂/CdS, TiO₂/Fe₂O₃ composites was successfully carried out by a number of simple techniques, such as hydrothermal deposition and electrochemical synthesis. The study of photocatalytic properties of arrays of nanorods, nanoparticles and nanoplasts showed a comparable current density when irradiated with a light source. After surface modification of the structures of titanium dioxide with nanoparticles of narrow-band semiconductor materials, the similarity of the photocurrent values disappears. Thus, the general picture of the increase in the photocurrent density confirms the positive effect of the decoration of structures by narrow-band semiconductor materials on the photoelectrochemical processes of the cell. Decoration of wide-gap semiconductor materials by layers of hematite also favourably contributed to an increase in the efficiency of the cell as a whole, which confirms the theory of band transitions in semiconductors and creates prerequisites for further work in the band engineering of semiconductor composites.

References

- [1] Fujishima A Electrochemical evidence for the mechanism of the primary stage of photosynthesis 1971 Book (Editor Bulletin of the chemical society of Japan) pp 1148-1150
- [2] Maeda K, Domen K New non-oxide photocatalysts designed for overall water splitting under visible light 2007 Journal of Physical Chemistry C 111 22 pp 7851-7861
- [3] Ismail A A, Bahnemann D W Photochemical splitting of water for hydrogen production by photocatalysis: A review 2014 Solar Energy Materials and Solar Cells 128 pp 85-101
- [4] Wolcott A Smith W A, Kuykendall T R, Zhao Y P, Zhang J Z Photoelectrochemical study of nanostructured ZnO thin films for hydrogen generation from water splitting 2009 Advanced Functional Materials 19, 12 pp 1849-1856
- [5] Shankar K, Basham J I, Allam N K, Varghese O K, Mor G K, Feng X J, Paulose M, Seabold J A, Choi K S, Grimes C A recent advances in the use of TiO₂ nanotube and nanowire arrays for oxidative photoelectrochemistry 2009 Journal of Physical Chemistry C 113, 16 pp 6327-6359
- [6] Hartmann P, Lee D K, Smarsly B M, Janek J Mesoporous TiO₂: comparison of classical Sol-Gel and nanoparticle based photoelectrodes for the water splitting reaction 2010 Acs Nano 4, 6 pp

3147-3154

- [7] Szymanski P, El-Sayed M A Some recent developments in photoelectrochemical water splitting using nanostructured TiO₂: a short review 2012 Theoretical Chemistry Accounts 131, 6
- [8] Park J. H, Kim S, Bard A J Novel carbon-doped TiO₂ nanotube arrays with high aspect ratios for efficient solar water splitting 2006 Nano Letters 6 1 pp 24-28
- [9] Tang J W, Durrant J R, Klug D R Mechanism of photocatalytic water splitting in TiO₂ reaction of water with photoholes, importance of charge carrier dynamics, and evidence for four-hole chemistry 2008 Journal of the American Chemical Society 130 42 pp 13885-13891

Репозиторий КарГУ